

# Optimize the Unseen - Fast NeRF Cleanup with Free Space Prior

Leo Segre      Shai Avidan

Tel Aviv University

<https://leosegre.github.io/optimize-the-unseen/>

## Abstract

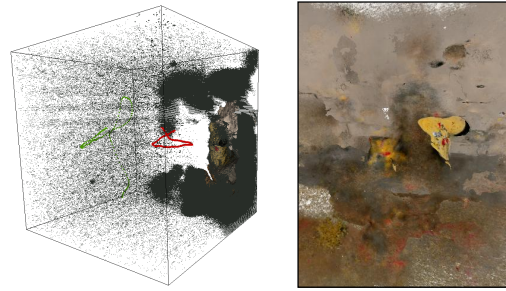
Neural Radiance Fields (NeRF) have advanced photorealistic novel view synthesis, but their reliance on photometric reconstruction introduces artifacts, commonly known as "floaters". These artifacts degrade novel view quality, especially in areas unseen by the training cameras. We present a fast, post-hoc NeRF cleanup method that eliminates such artifacts by enforcing our Free Space Prior, effectively minimizing floaters without disrupting the NeRF's representation of observed regions. Unlike existing approaches that rely on either Maximum Likelihood (ML) estimation to fit the data or a complex, local data-driven prior, our method adopts a Maximum-a-Posteriori (MAP) approach, selecting the optimal model parameters under a simple global prior assumption that unseen regions should remain empty. This enables our method to clean artifacts in both seen and unseen areas, enhancing novel view quality even in challenging scene regions. Our method is comparable with existing NeRF cleanup models while being  $2.5\times$  faster in inference time, requires **no additional memory** beyond the original NeRF, and achieves cleanup training in less than 30 seconds. Our code will be made publically available.

## 1. Introduction

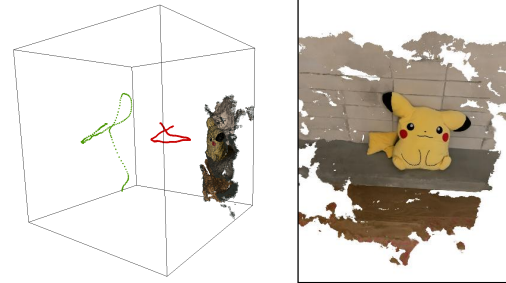
Neural Radiance Fields (NeRF) have emerged as a leading technique in photorealistic scene reconstruction and novel view synthesis, effectively capturing complex scenes from a limited set of images. However, NeRF's reliance on photometric optimization introduces a significant limitation: it performs poorly in regions of the scene that lack direct observations from the training images. This results in visual artifacts, commonly referred to as "floaters," which are density accumulations in areas unseen by the training cameras. These floaters degrade rendering quality, especially in novel views where the artifacts may obscure scene surfaces or introduce false details, as illustrated in Figure 1.

While state-of-the-art approaches for NeRF cleanup can

## Pre-Trained NeRF



Novel View



## Free Space Prior NeRF

Figure 1. **Density Cleanup:** Areas unseen by training rays lack optimization, leading to artifacts and "floaters". To demonstrate this, we sampled densities uniformly within the bounding box  $[-1, 1]$ , generating a point cloud of regions with densities above a threshold. Training cameras marked in red and evaluation cameras marked in green. The Top scene highlights significant floater artifacts, especially behind training cameras where rays are absent, which can degrade novel view quality. Our approach, as shown on the bottom, effectively removes these artifacts by optimizing densities even in unseen regions, resulting in cleaner novel views.

mitigate artifacts, they often come with a high computational cost. Nerfbusters [26] uses 3D diffusion models to generate a learned, data-driven 3D prior, necessitating

NeRF fine-tuning and resulting in substantial computational demands and extended cleanup training time. BayesRays [8], an alternative approach, reduces training time by performing post-hoc uncertainty-based cleanup; however, it introduces considerable overhead at inference due to continuous uncertainty estimation. These approaches highlight a key trade-off in existing methods between efficient artifact removal and computational expense, underscoring the need for a more effective solution.

Current methods follow either a Maximum Likelihood (ML) approach, optimizing model parameters to fit the observed data, or rely on a complex, data-driven local prior to match a general data distribution. We, in contrast, take a Maximum-a-Posteriori (MAP) approach with a simple global prior. Where, among all possible models that can explain the data, we seek the one that also satisfies the prior assumption.

We introduce a novel, post-hoc method that cleans up artifacts in pre-trained NeRFs without altering the core NeRF architecture or adding any extra computation during inference. Similarly to Gaussian Splatting [11], that ideally models only visible regions by assuming unobserved regions to be empty, our method applies this assumption to NeRF. In practice, however, Gaussian Splatting can still suffer from artifacts, and NeRF is even more prone to unwanted density accumulations ("floaters") in unseen areas. By explicitly optimizing these regions in NeRF, our method reduces floaters and improves scene quality, outperforming even Gaussian Splatting in cleanup.

Our method samples across the entire 3D space, applying a Free Space Prior that enforces zero density in regions unobserved by training rays. Our method is designed to be lightweight and efficient: we only fine-tune the NeRF itself, without training additional networks or increasing inference-time memory and computation. This ensures that floaters are minimized without disrupting the scene's intended structure or introducing additional memory requirements. The method is both efficient and highly compatible with existing NeRF cleanup models, offering a significant improvement in speed and memory efficiency compared to state-of-the-art artifact removal techniques. The contributions of our method are summarized as follows:

- **Efficiency in computation and memory:** Our approach requires **no additional memory** beyond the original NeRF, is **2.5x faster** in inference time, and **1.5x faster** in cleanup train time to current SOTA methods.
- **State-of-the-art artifact removal:** Our method achieves high-quality NeRF cleanup by effectively eliminating floaters, leading to more accurate novel view synthesis.
- **Optimization in unseen regions:** Unlike previous methods that focus solely on regions observed by training cameras, our method also optimizes density in unseen regions, reducing artifacts throughout the scene.

## 2. Related Works

Neural Radiance Fields (NeRFs) [17] often exhibit visual artifacts, such as "floaters" and density inconsistencies, due to training data imperfections, including incomplete scene coverage and data noise. These issues introduce uncertainties in unobserved regions, which can be divided into **aleatoric** and **epistemic** uncertainty.

Aleatoric uncertainty, arising from data noise like lighting changes or transient objects, has been addressed in dynamic scenes by works such as NeRF-W [13] and others [9, 20, 21]. In contrast, our focus is on static scenes with epistemic uncertainty, stemming from incomplete scene information. Approaches like CF-NeRF [23] use variational inference to capture this uncertainty in geometry, while BayesRays [8] applies a Bayesian framework to estimate epistemic uncertainty post-training. Our work specifically addresses cleanup of artifacts in static scenes caused by epistemic uncertainty.

**Artifacts in Photometric Optimization** Methods based on photometric reconstruction [15, 16], such as NeRF [17] and 3D Gaussian Splatting [11], have become leading techniques in 3D reconstruction due to their ability to generate high-quality, detailed scene representations by modeling the scene from multi-view images. These methods excel in reconstructing complex geometry and capturing subtle visual details by leveraging the information embedded in photometric data. However, due to their reliance on photometric reconstruction, which inherently contains uncertainties stemming from incomplete or noisy input data, these methods are prone to visual artifacts. While artifacts in Gaussian Splatting typically concentrate around scene structures due to imperfect Gaussian optimization [29, 32], NeRF artifacts are more widely distributed across the scene, often impacting novel views severely.

**NeRF Cleanup.** Various methods have been proposed to address the visual artifacts common in NeRF reconstructions. For example, Nerfbusters [26] introduced a post-processing technique using diffusion models that learns a local 3D data-driven prior from synthetic data. This data-driven prior, incorporated during NeRF optimization, encourages plausible geometry but requires extensive training and NeRF fine-tuning, adding significant computational overhead. Another approach, BayesRays [8], leverages a post-hoc solution by thresholding an uncertainty field to mask high-uncertainty regions, effectively cleaning artifacts at inference time but at the cost of increased computation during rendering.

These methods, though effective, often come with trade-offs in memory consumption, training time, or inference speed. In contrast, our approach removes artifacts effi-

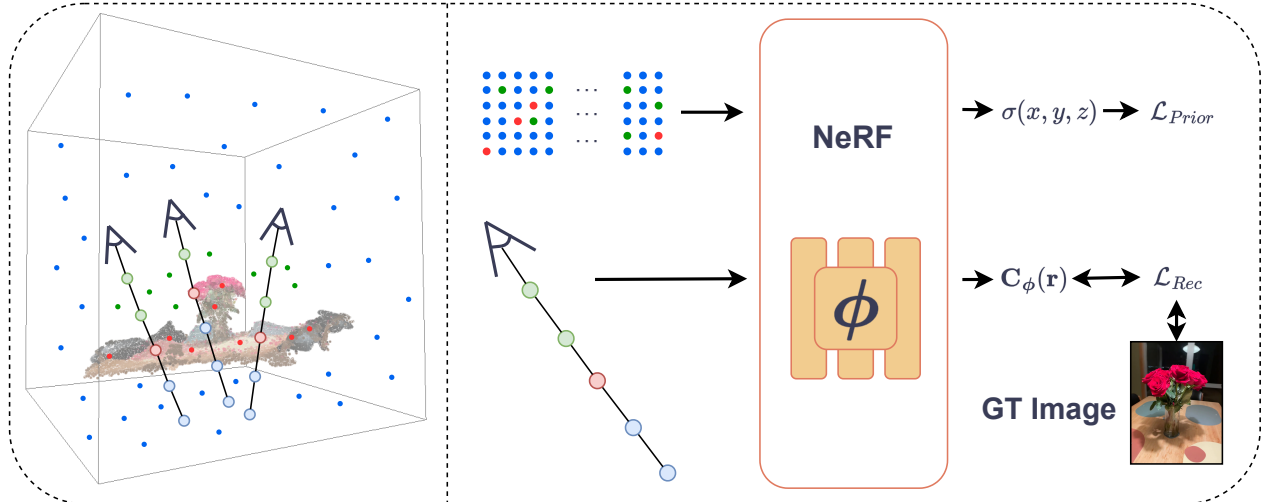


Figure 2. **Architecture Overview:** Our method fine-tunes a pre-trained NeRF to clean artifacts. During each optimization step, we simultaneously optimize two objectives: (1) density is optimized using our Free Space Prior across randomly sampled 3D points, enforcing zero density in all regions, and (2) the NeRF reconstruction loss is optimized along the original training images. For clarity, the points are grouped by region: blue points represent areas unseen by the training cameras, while green and red points are seen by the training cameras. Green points lie between the camera and the object, while red points are located on the object surface. Note that blue points may also appear along camera rays due to occlusions.

ciently, preserving the original NeRF’s structure and performance without requiring additional models or extensive post-processing, based only on our Free Space Prior. This ensures both speed and practicality in artifact cleanup.

**Prior-Based Optimization** Data-driven optimization is standard in deep learning, but numerous studies demonstrate that incorporating a well-chosen prior can significantly boost performance. For instance, priors have proven effective in inverse problems like image denoising [4–6, 10, 22, 28]. In particular, [5, 6] introduce a global image prior enforcing sparsity, showcasing how a Bayesian framework can yield a simple yet powerful denoising algorithm. In the context of 3D reconstruction, priors and regularization play similarly critical roles. Nerfbusters [26] uses a local prior to improve scene fidelity and and RegNeRF [19] employs a 2D Total Variation (TV) regularizer to rendered images, both maintaining the standard NeRF architecture as we do. Other methods modify the architecture. For example, Plenoxels [30] employs a 3D Total Variation (TV) regularizer to reduce abrupt density changes between neighboring voxels and 2D TV regularization is also applied in factorized plenoptic fields [3, 7]. Plenotrees [31] incorporates a sparsity loss within a complex pipeline for faster rendering but at high memory and training costs. Alternatively, mip-NeRF 360 [2] applies a distortion loss to penalize regions with high photometric error, offering regularization that reduces artifacts and enhances model consistency.

Inspired by the above, our method employs a global prior

to enforce free space within NeRF 3D scenes, enhancing NeRF’s rendering performance.

### 3. Background

We propose a method for cleaning artifacts in Neural Radiance Fields (NeRF) by addressing the limitations of conventional photometric optimization. Our approach leverages the strengths of photometric optimization to preserve the scene’s integrity while effectively eliminating artifacts. Understanding NeRF is essential to grasp the significance of our work and its contributions to the field. In this section, we review the fundamental concepts of NeRF and discuss the challenges associated with artifact generation in unobserved regions, which our approach aims to overcome.

#### 3.1. Neural Radiance Fields

Neural Radiance Fields (NeRF) [17] represent an approach for synthesizing novel views of complex 3D scenes. In NeRF, each point in 3D space is represented by a view-dependent radiance and a view-independent density value, mathematically expressed as follows:

$$\mathbf{c}_\phi(\mathbf{x}, \mathbf{d}), \tau_\phi(\mathbf{x}) = \mathcal{R}(\mathbf{x}, \mathbf{d}; \phi) \quad (1)$$

Here,  $\phi$  denotes the learnable parameters of the neural network. The color of each pixel in the rendered image is computed through volume rendering techniques, where the color along a ray  $\mathbf{r} = \mathbf{o}_r + t \cdot \mathbf{d}_r$  is determined by sampling points  $t_i$  along the ray:

$$\mathbf{C}_\phi(\mathbf{r}) = \sum_i \exp\left(-\sum_{j<i} \tau_j \delta_j\right) (1 - \exp(-\tau_i \delta_i)) \mathbf{c}_i, \quad (2)$$

In this equation,  $\delta_i$  represents the distance between successive sampled points. The optimization of the network parameters  $\phi$  aims to minimize the reconstruction loss, which is defined as the squared distance between the predicted and ground truth colors for each ray sampled from the training images  $R = \{\mathbf{r}\}_{n=0}^N$ .

$$\mathcal{L}_{\text{rec}} = \sum_{\mathbf{r} \in R} \|\mathbf{C}_\phi(\mathbf{r}) - \mathbf{C}_n^{\text{gt}}(\mathbf{r})\|_2^2 \quad (3)$$

An important observation from Equation (2) is that NeRF’s optimization occurs on a per-pixel basis, with the color of each pixel computed along a single ray. Since density decreases exponentially along the ray after it intersects the first surface, there is effectively no optimization beyond that surface, and certainly none where the ray does not pass through. Consequently, unseen regions remain unoptimized, often resulting in unwanted artifacts in these areas.

## 4. Method

Our goal is to eliminate floater artifacts in NeRF reconstructions while preserving the structural integrity of the scene. Our approach, as shown in our architecture Figure 2, is designed as a post-hoc refinement, takes a pre-trained NeRF model along with its training cameras and optimizes it to remove artifacts in unseen regions while retaining the scene’s intended features.

To date, NeRF models, and NeRF cleanup methods in particular, searched for a density field  $\sigma$  that best explains the given data. That is, They look for the maximum likelihood solution to the problem. Some methods extend this by learning a general data distribution over multiple 3D scenes, creating a local prior for artifact removal. In contrast, we apply a simple, global prior on the density  $\sigma$  - We take the prior  $P(\sigma)$  to be the zero density prior.

**Optimizing the Unseen** NeRF excels at minimizing photometric loss over the training images, providing accurate reconstructions in observed areas. However, it does not constrain unseen regions, often resulting in noisy artifacts, or “floaters,” in those areas. We base our method on the prior assumption that “There is nothing in the unseen regions.” While this assumption does not necessarily hold in real-world scenarios, for NeRF reconstructions, it is more practical than allowing unseen regions to contain unregulated noise. To enforce this assumption, we apply a sigmoid-softened density prior term that gently drives density  $\sigma$  toward zero:

$$\text{sigmoid}(\sigma) = \frac{1}{1 + e^{-\sigma}} \quad (4)$$

**Enforcing the Free Space Prior** Ideally, we would like to directly set densities to zero only in the unseen regions. However, determining which regions are strictly unobserved by training rays is challenging due to scene occlusions and structural complexity. Additionally, even if feasible, this direct approach would be computationally expensive. rather than explicitly setting densities, we apply the Free Space Prior uniformly across the entire 3D space, affecting both seen and unseen regions. This approach simplifies computation while guiding NeRF optimization to achieve cleaner density distributions.

To implement this, we randomly sample  $\mathcal{N}$  points across the 3D space and query the NeRF model  $\phi$  for densities at these points, resulting in a set  $\Sigma = \{\sigma(\mathbf{x}_i) \mid \mathbf{x}_i \in \mathbb{R}^3, i = 1, \dots, \mathcal{N}\}$  of density values. We then construct a softened density term for the Free Space Prior, as shown in Equation (4), which we integrate into a Free Space Prior Loss term:

$$\mathcal{L}_{\text{FSP}} = \sum_{i=1}^{\mathcal{N}} \left( \frac{1}{1 + e^{-\sigma(\mathbf{x}_i)}} \right)^2 \quad (5)$$

This Free Space Prior Loss optimizes the NeRF parameters  $\phi$  by enforcing densities to be zero, reflecting our assumption that “There is nothing in the unseen regions.” However, this loss also inadvertently reduces densities in seen regions, where densities should ideally reflect the actual scene structure.

**Clean While Preserve** Applying the Free Space Prior Loss indiscriminately across 3D space can lead to an empty scene, as the randomly enforced zero-density constraint propagates, causing the MLP to approximate densities as zero throughout the space. To counter this, we introduce a combination of two competing losses: the Free Space Prior Loss Equation (5) to reduce densities in unseen regions and the NeRF photometric loss Equation (3) applied along training rays to preserve the scene structure and appearance.

This interaction between losses results in three distinct regions:

- **Unseen Regions:** Only the Free Space Prior Loss affects these regions, pushing densities toward zero and removing floaters.
- **Empty Seen Regions (along the ray to the surface):** Both the Free Space Prior Loss and the photometric loss act here, agreeing that the density should be zero.
- **Surface Seen Regions:** Both losses are active, but they compete, as the Free Space Prior Loss encourages lower densities while the photometric loss preserves the actual scene structure.



Figure 3. **Qualitative Cleanup Results:** Visualization of different cleanup methods applied to the Plant and Roses scenes from the Nerfbusters dataset. Each image shows a novel view from the evaluation set rendered post-cleanup. The comparison highlights each method’s effectiveness in balancing artifact removal with scene coverage. These visual results correspond to Figure 4 and illustrate the concept of coverage: methods such as Free Space Prior and BayesRays with a 0.9 threshold yield high coverage with minimal artifacts, while Nerfbusters and BayesRays with a 0.3 threshold result in lower coverage, with varying degrees of artifact cleanup. For comparison, we also provide in the last column the results of Gaussian Splatting.

Through this balanced combination, empty regions will ultimately reach zero density, eliminating floaters. In contrast, surface regions will settle on a density value that balances both losses, resulting in a reduced yet preserved density that maintains accurate scene reconstruction, as shown in our experiments.

The overall loss function for our method is a weighted combination of these two terms, where  $\lambda$  acts as a temperature parameter, controlling the aggressiveness of the cleanup process.

$$\mathcal{L} = \mathcal{L}_{\text{rec}} + \lambda \mathcal{L}_{\text{prior}} \quad (6)$$

To summarize, our method provides an efficient solution for NeRF artifact cleanup by applying a Free Space Prior to unseen regions, effectively eliminating floaters without adding extra networks or computations during inference. By fine-tuning the pre-trained NeRF, we achieve significant cleanup with minimal computational overhead. The combination of the Free Space Prior loss and photometric loss allows for effective removal of artifacts while preserving the scene structure, making our method faster and more memory-efficient compared to existing approaches. Our experiments demonstrate that this approach maintains high-quality scene reconstruction with reduced training and inference times.

## 5. Results

We evaluate our NeRF cleanup method by analyzing performance in the NeRF cleanup task, comparing both quan-

titative metrics and inference speed. We report numerical results to quantify the reduction of artifacts (floaters) and demonstrate that our approach achieves substantial speedup while maintaining high output quality. Qualitative visualizations further illustrate the effectiveness of our artifact removal process, highlighting that our method not only accelerates the rendering but also preserves or enhances scene fidelity. Additionally, we include ablation studies to assess the impact of key components in our design, offering deeper insights into their contributions to artifact cleanup performance.

### 5.1. Dataset and Evaluation Setup

We evaluate the effectiveness of our method in removing artifacts—referred to as “floaters”—from NeRF reconstructions, following the experimental protocols established by Nerfbusters [26] and BayesRays [8]. Our goal is to assess each method’s ability to eliminate these artifacts while preserving the quality and completeness of the reconstructed scenes. For this evaluation, we utilize the Nerfbusters dataset [26], designed specifically for benchmarking NeRF cleanup methods. This dataset presents challenging scenes for NeRF-based reconstructions, providing an ideal testing ground for artifact removal effectiveness. To gauge performance, we report PSNR and Coverage scores, which quantify reconstruction quality and the extent to which the scene is accurately rendered without artifacts, respectively.

We introduce a key modification to the original experiment to make the task more realistic and challenging. Pre-

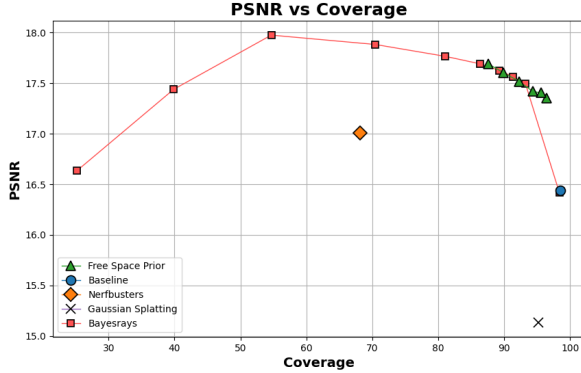


Figure 4. **Quantitative Cleanup Results:** This plot compares the cleanup performance of various methods using PSNR as a function of Coverage across different thresholds (if applicable). Higher PSNR and Coverage scores represent better performance, with the optimal region located at the upper-right, where both metrics are maximized. For our method, each point reflects the effect of varying cleanup aggressiveness, controlled by the  $\lambda$  parameter from Equation (6). Measurements are averaged across all scenes in the Nerfbusters dataset to ensure a comprehensive comparison. We also provide results of Gaussian Splatting for reference.

vious experiments calculated PSNR, SSIM and LPIPS over the **ground truth (GT) mask**, which only considers the object region. This can overestimate performance, as artifacts outside the GT mask are ignored. In our setup, PSNR is calculated over the **predicted mask**, penalizing methods that leave artifacts outside the GT mask. This provides a stricter evaluation, ensuring that methods are assessed on their ability to remove artifacts while maintaining scene integrity.

**Coverage Metric** We adopt the coverage metric as introduced by Nerfbusters [26], which measures the percentage of pixels in the evaluation image that are accurately reconstructed after masking out regions that were either unseen in the training views or are too distant to be relevant (based on a predefined depth threshold).

**Implementation Details** All experiments were conducted using the latest version of Nerfacto and Splatfacto from Nerfstudio [25], pre-trained for 30,000 steps. Comparisons between different methods were performed on the same pre-trained base NeRF model to ensure consistency. In our method, density optimization was achieved with 1,000 iterations using  $2^{17}$  randomly sampled points across the 3D scene space. Optimization was carried out through Nerfacto’s optimizers. All experiments were run on a single NVIDIA RTX A5000 GPU. Results for BayesRays [8] and Nerfbusters [26] were generated using their respective pipelines, including the pre-trained 3D diffusion model weights provided by Nerfbusters. The Nerfacto model we

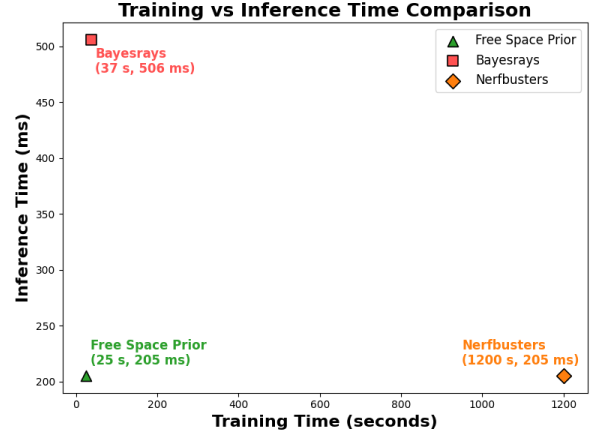


Figure 5. **Runtime Comparison:** Training runtime Vs Inference runtime per frame. This plot compares the runtime performance of three cleanup methods. The inference time is measured in milliseconds per frame, averaged across all scenes in the Nerfbusters dataset. Note that both Nerfbusters and Free Space Prior methods only involve the finetuned NeRF during inference, resulting in the same inference time for both.

used incorporates recent advancements in NeRFs, including hash grid encoding [18], proposal sampling and scene contraction [1], as well as per-image appearance optimization [14]. The splatfacto model is based on Gaussian Splatting [11] with regularization to prevent artifacts [27, 29].

## 5.2. Performance Comparison

In this section, we assess the effectiveness of our NeRF cleanup method in comparison to state-of-the-art approaches, focusing on both artifact removal quality and computational efficiency. We evaluate performance through quantitative metrics such as PSNR and Coverage, as well as runtime efficiency, considering both training and inference times. Our method is designed to maximize the trade-off between image quality and coverage while providing significant speed advantages.

**Cleanup Performance** Our method achieves competitive results with significantly faster training and inference times, as shown in Figure 5. In Figure 4, our approach demonstrates high coverage while maintaining a PSNR comparable to BayesRays, the current state-of-the-art in NeRF cleanup. Striking a balance between high PSNR and high coverage is crucial, as high PSNR with low coverage can be misleading, as illustrated, as shown in Figure 3. For instance, BayesRays at a 0.3 threshold achieves the highest PSNR on the graph but suffers from low coverage, leading to noticeable gaps in the reconstructed scene that compromise overall image quality. In contrast, both the Nerfacto baseline and Gaussian Splatting models exhibit excel-

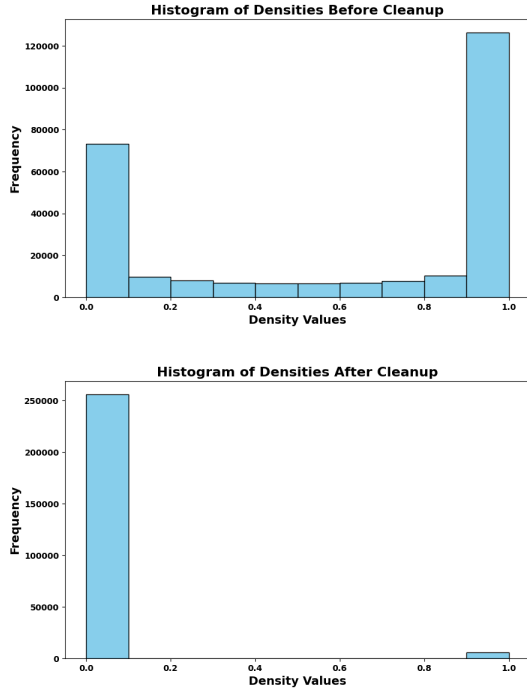


Figure 6. **Density Histogram:** Histogram of densities across the Pikachu scene after sigmoid-softened as in Equation (4), shifted to  $[0, 1]$  (Top) Histogram of densities across the scene before the cleanup process (Bottom) Histogram of the densities across the scene after the cleanup process.

lent coverage but lower PSNR, underscoring the challenge posed by the dataset, which is designed to test these specific issues. Artifacts such as density accumulation in Nerfacto and scattered Gaussians in Gaussian Splatting are also clearly visible.

Our method, as well as BayesRays with a 0.9 threshold, produces visually superior results that retain the scene’s structure and coverage, making them more visually appealing and accurate to a human eye. These images highlight that our method preserves both high coverage and high PSNR, outperforming Nerfbusters, which, while comparable in inference, achieves lower PSNR and coverage than our method. Overall, our method achieves the best coverage, surpassed only by the baseline, but with substantially higher PSNR, confirming its effectiveness in both artifact removal and scene fidelity.

**Runtime Performance** Our method combines fast training and inference times Figure 5 while maintaining high-quality artifact cleanup Figure 3. For inference, both Nerfbusters and our method achieve a per-frame rendering time of 205 ms, as each directly fine-tunes the NeRF without adding additional overhead at inference. In contrast,

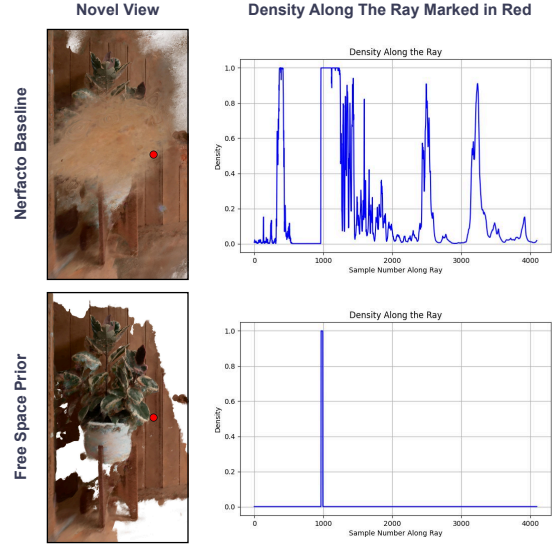


Figure 7. **Density Along a Ray:** (Left) Novel views of the Plant scene, rendered with the Nerfacto Baseline and our Free Space Prior, with a red dot marking the sampled ray shown in the graph. (Right) Graph of density along the marked ray. Before cleanup, the density field is noisy, while after cleanup it captures only the surface along the ray. In the baseline densities, the first peak corresponds to the floater seen in the image, the second peak to the wall (present in both images and graphs), and the subsequent unseen regions, which are noisy in the baseline, are enforced to zero after cleanup. Densities are softened using Equation (4) and shifted to  $[0, 1]$

BayesRays incurs a significant slowdown, with a per-frame inference time of 506 ms—2.5 times slower—due to its additional uncertainty thresholding applied during rendering.

For training time, Nerfbusters employs a pre-trained 3D diffusion model to fine-tune NeRF per scene, resulting in a high training time of approximately 20 minutes per scene. BayesRays is faster, taking 37 seconds to gather data for Hessian computation, while our approach is the fastest, completing cleanup training in just 25 seconds.

**Overall Performance** Our NeRF cleanup method demonstrates a well-rounded balance of high-quality artifact removal, high scene coverage, and rapid computational performance. Compared to existing methods, it achieves similar or superior visual results with notably reduced training times and maintains efficient inference speeds on par with the baseline NeRF model. These results underscore the practicality of our approach for applications where both visual fidelity and speed are critical. The combination of efficient cleanup and low runtime costs illustrates our method’s capability to enhance NeRF-based scene reconstructions without the need for extensive additional resources.

### 5.3. Ablation Study

First, we examine the effect of our method on the density distribution in the scene, comparing density histograms before and after cleanup. This analysis helps us understand how our approach distinguishes between object surfaces and empty space, ultimately refining the NeRF’s representation of the scene. Second, we test our hypothesis that sampling across the entire 3D space, especially in unseen regions, is crucial for effective artifact removal. We conduct experiments to compare our random sampling strategy with sampling exclusively along training rays, evaluating the effect on cleanup quality. Together, these studies provide insights into why our method succeeds in both comprehensive artifact removal and scene preservation.

**Densities Histogram** We analyzed density distributions across the scene before and after applying our cleanup method, by measuring the densities in random  $2^{18}$  points across the scene space, visualized in Figure 6. Before cleanup, the density histogram shows three distinct ranges: high densities representing object surfaces and floaters, intermediate densities indicating regions with inconsistent optimization from the NeRF training, and zero densities corresponding to empty space. The presence of intermediate densities highlights that regions outside the training camera views received little to no regularization during the NeRF training, allowing densities to vary without specific constraints.

After cleanup, the density distribution shifts to a bimodal pattern, effectively removing intermediate values and clustering densities around zero or high values. This shift indicates that our method enforces a clear distinction between object and empty space, aligning the density distribution more closely with an ideal NeRF scene representation. The majority of the densities now approach zero, with only a small fraction remaining high to capture object surfaces. This refined distribution improves the NeRF’s alignment with real scene structures, as illustrated in Figure 1. As shown in Figure 7, the post-cleanup distribution clearly demonstrates this shift, with the intermediate densities largely eliminated and a more concentrated focus on the object and empty space densities.

**Sampling Along Training Rays** In our approach, we apply the Free Space Prior Loss Equation (5) by sampling randomly across the entire 3D scene space, which includes both seen and unseen regions. We hypothesize that sampling in unseen areas is crucial to effectively removing artifacts and achieving high-quality novel views. To validate this, we conducted an ablation study comparing our method with a setup in which the Loss is applied only to densities sampled along the training rays. These rays pass through

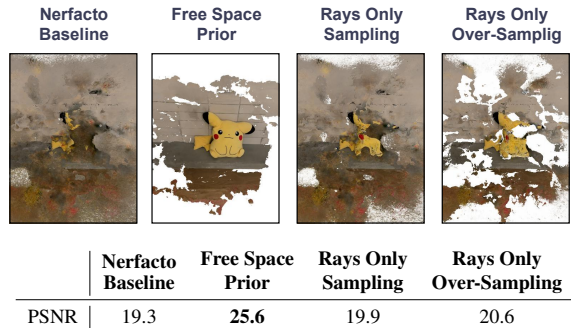


Figure 8. **Applying the Prior Along Training Rays:** Ablation study on applying the Free Space Prior loss specifically along the training rays, with varying numbers of samples per ray. (Top) Visualizations show the cleanup results for each method on a novel view. (Bottom) The PSNR score for each method, averaged over the Pikachu scene evaluation set, demonstrate the quantitative impact of sampling along training rays.

seen regions and some unseen areas directly behind objects, but do not cover all unseen areas (as illustrated in Figure 2).

In this study, we tested two variations limited to ray-based sampling. The first used 32 samples per ray across 4,096 rays, matching the 131,072 samples of our original method. The second increased samples to 512 per ray, totaling 2,097,152 points per iteration. Figure 8 show that our random sampling achieves a PSNR of 25.6, significantly surpassing ray-based methods. Sampling with 32 samples per ray raised PSNR from 19.3 to 19.9, while 512 samples per ray improved it to 20.6, though artifacts persisted, and some scene details were lost due to over-aggressive cleanup.

These findings confirm that sampling the full 3D space is essential for effective artifact removal, as ray-based sampling misses unseen regions, resulting in incomplete cleanup or loss of scene detail.

## 6. Conclusion

we present an efficient post-hoc cleanup method for Neural Radiance Fields (NeRFs) that is based on a simple Free Space Prior, and show that it significantly reduces artifacts, specifically floaters, in unseen regions of a scene. Our approach stands out due to its ability to eliminate these artifacts without modifying the core NeRF architecture or adding additional memory overhead, offering a solution that is both fast and scalable. We have demonstrated that our method outperforms state-of-the-art approaches in terms of both efficiency and quality. Specifically, our method achieves up to  $2.5\times$  faster inference time,  $1.5\times$  faster train time and requires no additional memory. It maintains high fidelity in the reconstructed scene, making it a practical choice for real-world applications.



## 7. Supplementary

### 7.1. Method Robustness

The Nerfbusters dataset [26] is specifically designed to test the cleanup task with challenging evaluation camera positions, making it an excellent benchmark for assessing artifact removal. However, the floater artifact phenomenon is not unique to Nerfbusters—it is a common issue across NeRF scenes. The primary limitation of other datasets is the lack of challenging evaluation cameras that can serve as a reliable ground truth for cleanup assessment.

To demonstrate the robustness and generalizability of our method, we evaluate it qualitatively on scenes from other widely used datasets. Specifically, we include results for the Garden scene from the mip-NeRF 360 dataset [2], the Basket scene from the Light Fields (LF) dataset [33], the Playground scene from the Tanks and Temples dataset [12], and the Trevi scene from the PhotoTourism dataset [24]. These scenes provide diverse settings with varying levels of complexity, testing the adaptability of our approach.

In Figure 9, and the attached videos, we compare our method to the Nerfacto baseline. The results confirm that our method effectively removes artifacts while preserving scene details across a wide range of scenes, underscoring its robustness beyond the Nerfbusters dataset.

### 7.2. Full Quantitative Results

Table 1 presents the complete evaluation results for all methods, directly correlating with the points depicted in Figure 4 of the main paper. Each row in Table 1 corresponds to a point in the PSNR vs. Coverage plot. Beyond the standard PSNR and Coverage metrics shown in the main paper, we also report SSIM, LPIPS, and Dice scores for a more comprehensive evaluation. While SSIM and LPIPS have been previously evaluated for BayesRays, we introduce the Dice score to provide additional insights into the cleanup results.

**Dice Score** To complement the coverage metric, we propose the Dice score as a meaningful addition for evaluating NeRF cleanup. The Dice score, widely used in segmentation tasks, quantifies the similarity between two sets by measuring their overlap. In the context of NeRF cleanup, it reflects how effectively a method removes unwanted artifacts. Specifically, it assesses how well a method distinguishes between the intended reconstruction and regions that should remain empty.

The Dice score offers a nuanced perspective that the coverage metric alone cannot provide. Coverage measures how completely a method reconstructs regions visible from the training cameras but does not penalize excessive retention of artifacts. In contrast, the Dice score penalizes methods that inaccurately retain content in unseen areas. For exam-

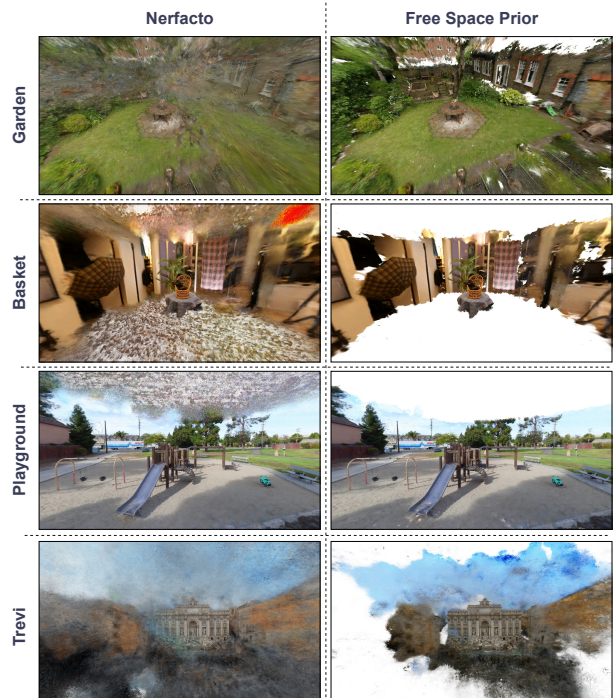


Figure 9. **Qualitative comparison of cleanup results on various scenes:** (Left) Novel view rendered using the Nerfacto model. (Right) The same view after applying our Free Space Prior cleanup. The evaluated scenes include **Garden** from the mip-NeRF 360 dataset, **Basket** from the Light Fields (LF) dataset, **Playground** from the Tanks and Temples dataset, and **Trevi** from the PhotoTourism dataset. Our method effectively removes artifacts while preserving scene details across diverse datasets.

Method	Threshold / $\lambda$	PSNR	SSIM	LPIPS	Coverage (%)	Dice
Nerfacto (Baseline)	N/A	16.44	0.53	0.45	98.48	0.83
Ours	$10^0$	17.69	0.62	0.30	87.57	0.87
	$10^{-1}$	17.60	0.60	0.32	89.88	0.88
	$10^{-2}$	17.52	0.58	0.35	92.26	0.89
	$10^{-3}$	17.42	0.57	0.37	94.35	0.90
	$10^{-4}$	17.40	0.56	0.39	95.60	0.90
	$10^{-5}$	17.35	0.56	0.40	96.45	0.90
Nerfbusters	N/A	17.01	0.64	0.27	68.13	0.73
BayesRays	0.1	16.64	0.70	0.19	25.21	0.43
	0.2	17.44	0.68	0.20	39.86	0.54
	0.3	17.97	0.67	0.23	54.67	0.65
	0.4	17.88	0.65	0.26	70.44	0.76
	0.5	17.77	0.63	0.28	81.04	0.83
	0.6	17.69	0.62	0.30	86.36	0.87
	0.7	17.63	0.61	0.32	89.27	0.88
	0.8	17.56	0.59	0.34	91.29	0.89
0.9	17.49	0.58	0.36	93.23	0.90	
1.0	16.42	0.53	0.45	98.36	0.82	
Gaussian Splatting	N/A	15.13	0.50	0.41	95.22	0.89

Table 1. **Full Results:** Comprehensive evaluation metrics for the methods discussed in our paper. Each row corresponds to a point in the PSNR vs. Coverage graph (Figure 4) from the main paper, providing additional insights into the trade-offs between reconstruction accuracy and artifact removal.

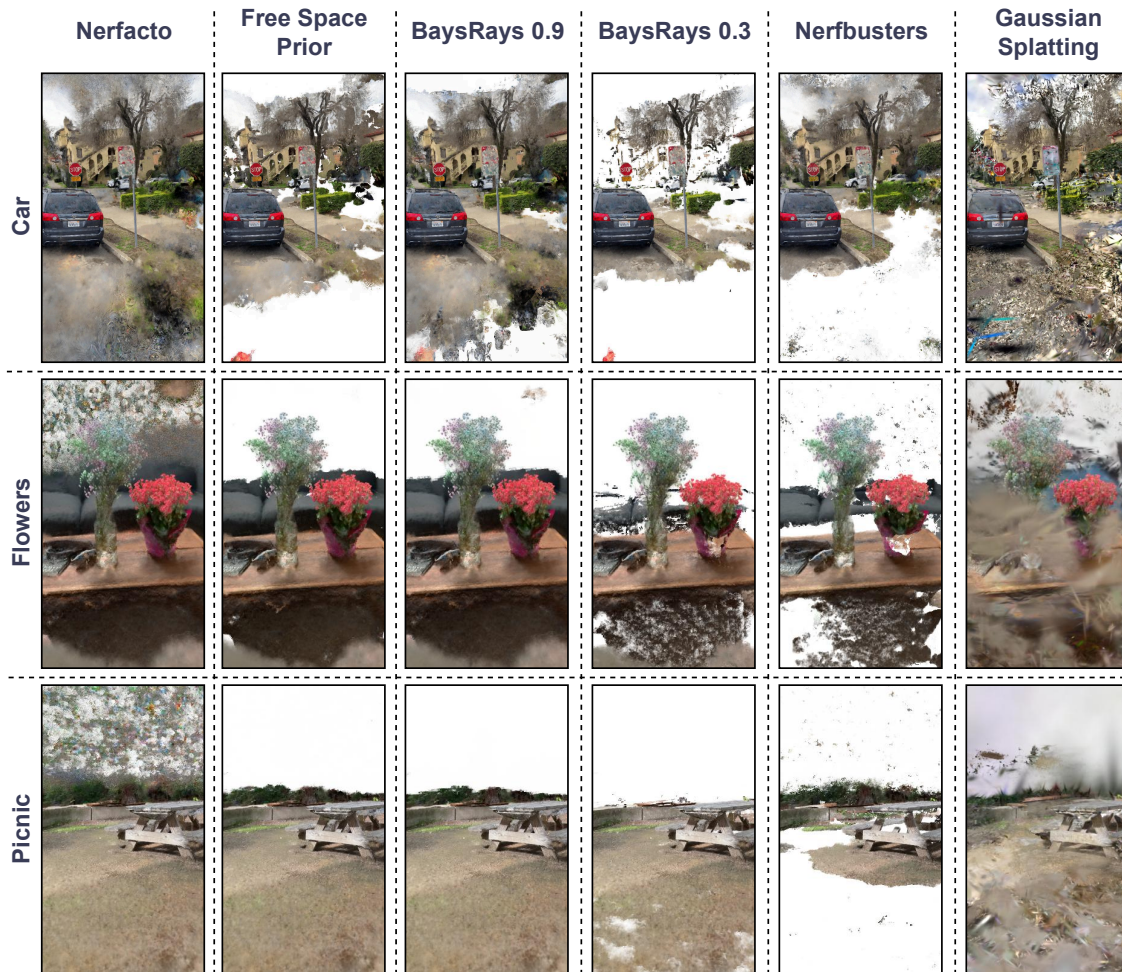


Figure 10. **Qualitative Cleanup Results:** Visualization of different cleanup methods applied to the Car, Flowers and Picnic scenes from the Nerfbusters dataset. Each image shows a novel view from the evaluation set rendered post-cleanup.

ple, as shown in Table 1, the baseline achieves a high coverage score because it does not perform any cleanup. However, Table 1 also reveals a low Dice score for the baseline, highlighting its inability to remove artifacts from unseen regions effectively.

This additional metric reinforces the importance of balancing reconstruction accuracy with artifact removal to achieve high-quality NeRF cleanups.

### 7.3. Additional Qualitative Results

We present qualitative results on additional scenes from the Nerfbusters dataset in Figure 10. These examples further support our claim of achieving a balance between effective cleanup and scene preservation. Our method demonstrates its ability to remove artifacts while maintaining the integrity

of the reconstructed regions, even in challenging scenarios.

Furthermore, the qualitative results highlight the limitations of Gaussian Splatting. Notably, it exhibits significant noise in novel views located far from the training cameras. This issue aligns with the quantitative findings, as the excessive noise contributes to the low PSNR scores reported in Table 1. These observations underline the importance of robust artifact removal in achieving high-quality reconstructions for novel viewpoints.

In addition to the static images, we attach videos of the Pikachu, Car, and Plant scenes from the Nerfbusters dataset. These videos provide side-by-side comparisons of the Nerfacto baseline and our Free Space Prior results. The comparisons clearly illustrate that our method delivers consistent artifact removal across the entire scene, rather than af-

fecting only isolated parts visible in the picked images. This consistency highlights our method’s robustness in addressing both local and global cleanup challenges while preserving the scene’s overall structure and quality.

## References

- [1] Jonathan T. Barron, Ben Mildenhall, Matthew Tancik, Peter Hedman, Ricardo Martin-Brualla, and Pratul P. Srinivasan. Mip-nerf: A multiscale representation for anti-aliasing neural radiance fields, 2021. 6
- [2] Jonathan T. Barron, Ben Mildenhall, Dor Verbin, Pratul P. Srinivasan, and Peter Hedman. Mip-nerf 360: Unbounded anti-aliased neural radiance fields. *CVPR*, 2022. 3, 9
- [3] Anpei Chen, Zexiang Xu, Andreas Geiger, Jingyi Yu, and Hao Su. Tensorf: Tensorial radiance fields, 2022. 3
- [4] Weisheng Dong, Peiyao Wang, Wotao Yin, Guangming Shi, Fangfang Wu, and Xiaotong Lu. Denoising prior driven deep neural network for image restoration. *IEEE Transactions on Pattern Analysis and Machine Intelligence*, 41(10):2305–2318, 2019. 3
- [5] M. Elad and M. Aharon. Image denoising via learned dictionaries and sparse representation. In *2006 IEEE Computer Society Conference on Computer Vision and Pattern Recognition (CVPR’06)*, pages 895–900, 2006. 3
- [6] Michael Elad and Michal Aharon. Image denoising via sparse and redundant representations over learned dictionaries. *IEEE Transactions on Image Processing*, 15(12):3736–3745, 2006. 3
- [7] Sara Fridovich-Keil, Giacomo Meanti, Frederik Warburg, Benjamin Recht, and Angjoo Kanazawa. K-planes: Explicit radiance fields in space, time, and appearance, 2023. 3
- [8] Lily Goli, Cody Reading, Silvia Sellán, Alec Jacobson, and Andrea Tagliasacchi. Bayes’ Rays: Uncertainty quantification in neural radiance fields. *CVPR*, 2024. 2, 5, 6
- [9] Liren Jin, Xieyuanli Chen, Julius Rückin, and Marija Popović. Neu-nbv: Next best view planning using uncertainty estimation in image-based neural rendering. In *2023 IEEE/RSJ International Conference on Intelligent Robots and Systems (IROS)*, pages 11305–11312, 2023. 2
- [10] Yeonsik Jo, Se Young Chun, and Jonghyun Choi. Rethinking deep image prior for denoising. In *Proceedings of the IEEE/CVF International Conference on Computer Vision (ICCV)*, pages 5087–5096, 2021. 3
- [11] Bernhard Kerbl, Georgios Kopanas, Thomas Leimkühler, and George Drettakis. 3d gaussian splatting for real-time radiance field rendering, 2023. 2, 6
- [12] Arno Knapitsch, Jaesik Park, Qian-Yi Zhou, and Vladlen Koltun. Tanks and temples: Benchmarking large-scale scene reconstruction. *ACM Transactions on Graphics*, 36(4), 2017. 9
- [13] Ricardo Martin-Brualla, Noha Radwan, Mehdi S. M. Sajjadi, Jonathan T. Barron, Alexey Dosovitskiy, and Daniel Duckworth. NeRF in the Wild: Neural Radiance Fields for Unconstrained Photo Collections. In *CVPR*, 2021. 2
- [14] Ricardo Martin-Brualla, Noha Radwan, Mehdi S. M. Sajjadi, Jonathan T. Barron, Alexey Dosovitskiy, and Daniel Duckworth. Nerf in the wild: Neural radiance fields for unconstrained photo collections, 2021. 6
- [15] N. Max. Optical models for direct volume rendering. *IEEE Transactions on Visualization and Computer Graphics*, 1(2): 99–108, 1995. 2
- [16] Ben Mildenhall, Pratul P. Srinivasan, Rodrigo Ortiz-Cayon, Nima Khademi Kalantari, Ravi Ramamoorthi, Ren Ng, and Abhishek Kar. Local light field fusion: Practical view synthesis with prescriptive sampling guidelines, 2019. 2
- [17] Ben Mildenhall, Pratul P. Srinivasan, Matthew Tancik, Jonathan T. Barron, Ravi Ramamoorthi, and Ren Ng. Nerf: Representing scenes as neural radiance fields for view synthesis. In *ECCV*, 2020. 2, 3
- [18] Thomas Müller, Alex Evans, Christoph Schied, and Alexander Keller. Instant neural graphics primitives with a multiresolution hash encoding. *ACM Transactions on Graphics*, 41(4):1–15, 2022. 6
- [19] Michael Niemeyer, Jonathan T. Barron, Ben Mildenhall, Mehdi S. M. Sajjadi, Andreas Geiger, and Noha Radwan. Regnerf: Regularizing neural radiance fields for view synthesis from sparse inputs, 2021. 3
- [20] Keunhong Park, Utkarsh Sinha, Jonathan T. Barron, Sofien Bouaziz, Dan B Goldman, Steven M. Seitz, and Ricardo Martin-Brualla. Nerfies: Deformable neural radiance fields. *ICCV*, 2021. 2
- [21] Yunlong Ran, Jing Zeng, Shibo He, Jiming Chen, Lincheng Li, Yingfeng Chen, Gimhee Lee, and Qi Ye. Neurar: Neural uncertainty for autonomous 3d reconstruction with implicit neural representations. *IEEE Robotics and Automation Letters*, 8(2):1125–1132, 2023. 2
- [22] Chao Ren, Xiaohai He, Chuncheng Wang, and Zhibo Zhao. Adaptive consistency prior based deep network for image denoising. In *Proceedings of the IEEE/CVF Conference on Computer Vision and Pattern Recognition (CVPR)*, pages 8596–8606, 2021. 3
- [23] Jianxiong Shen, Antonio Agudo, Francesc Moreno-Noguer, and Adria Ruiz. Conditional-flow nerf: Accurate 3d modelling with reliable uncertainty quantification, 2022. 2
- [24] Noah Snavely, Steven M. Seitz, and Richard Szeliski. Photo tourism: exploring photo collections in 3d. *ACM Trans. Graph.*, 25(3):835–846, 2006. 9
- [25] Matthew Tancik, Ethan Weber, Evonne Ng, Ruilong Li, Brent Yi, Justin Kerr, Terrance Wang, Alexander Kristoffersen, Jake Austin, Kamyar Salahi, Abhik Ahuja, David McAllister, and Angjoo Kanazawa. Nerfstudio: A modular framework for neural radiance field development. In *ACM SIGGRAPH 2023 Conference Proceedings*, 2023. 6
- [26] Frederik Warburg\*, Ethan Weber\*, Matthew Tancik, Aleksander Holyński, and Angjoo Kanazawa. Nerfbusters: Removing ghostly artifacts from casually captured nerfs. In *International Conference on Computer Vision (ICCV)*, 2023. 1, 2, 3, 5, 6, 9
- [27] Tianyi Xie, Zeshun Zong, Yuxing Qiu, Xuan Li, Yutao Feng, Yin Yang, and Chenfanfu Jiang. Physgaussian: Physics-integrated 3d gaussians for generative dynamics, 2024. 6
- [28] Jun Xu, Lei Zhang, and David Zhang. External prior guided internal prior learning for real-world noisy image denoising.

- IEEE Transactions on Image Processing*, 27(6):2996–3010, 2018. [3](#)
- [29] Zongxin Ye, Wenyu Li, Sidun Liu, Peng Qiao, and Yong Dou. Absgs: Recovering fine details for 3d gaussian splatting, 2024. [2](#), [6](#)
- [30] Alex Yu, Sara Fridovich-Keil, Matthew Tancik, Qinhong Chen, Benjamin Recht, and Angjoo Kanazawa. Plenoxels: Radiance fields without neural networks, 2021. [3](#)
- [31] Alex Yu, Ruilong Li, Matthew Tancik, Hao Li, Ren Ng, and Angjoo Kanazawa. Plenotrees for real-time rendering of neural radiance fields, 2021. [3](#)
- [32] Zehao Yu, Torsten Sattler, and Andreas Geiger. Gaussian opacity fields: Efficient adaptive surface reconstruction in unbounded scenes, 2024. [2](#)
- [33] Kaan Yücer, Alexander Sorkine-Hornung, Oliver Wang, and Olga Sorkine-Hornung. Efficient 3d object segmentation from densely sampled light fields with applications to 3d reconstruction. *ACM Trans. Graph.*, 35(3), 2016. [9](#)